

Discovery of two new Galactic candidate luminous blue variables with *Wide-field Infrared Survey Explorer**

V. V. Gvaramadze,^{1,2†} A. Y. Kniazev,^{1,3,4} A. S. Miroshnichenko,⁵ L. N. Berdnikov,^{1,2} N. Langer,⁶ G. S. Stringfellow,⁷ H. Todt,⁸ W.-R. Hamann,⁸ E. K. Grebel,⁹ D. Buckley,⁴ L. Crause,³ S. Crawford,^{3,4} A. Gulbis,^{3,4} C. Hettlage,^{3,4} E. Hooper,¹⁰ T.-O. Husser,¹¹ P. Kotze,^{3,4} N. Loaring,^{3,4} K. H. Nordsieck,¹⁰ D. O’Donoghue,⁴ T. Pickering,^{3,4} S. Potter,³ E. Romero Colmenero,^{3,4} P. Vaisanen,^{3,4} T. Williams,¹² M. Wolf,¹⁰ D. E. Reichart,¹³ K. M. Ivarsen,¹³ J. B. Haislip,¹³ M. C. Nysewander¹³ and A. P. LaCluyze¹³

¹Sternberg Astronomical Institute, Lomonosov Moscow State University, Universitetskij Pr. 13, Moscow 119992, Russia

²Isaac Newton Institute of Chile, Moscow Branch, Universitetskij Pr. 13, Moscow 119992, Russia

³South African Astronomical Observatory, PO Box 9, 7935 Observatory, Cape Town, South Africa

⁴Southern African Large Telescope Foundation, PO Box 9, 7935 Observatory, Cape Town, South Africa

⁵Department of Physics and Astronomy, University of North Carolina at Greensboro, Greensboro, NC 27402-6170, USA

⁶Argelander-Institut für Astronomie der Universität Bonn, Auf dem Hügel 71, 53121 Bonn, Germany

⁷CASA, University of Colorado, UCB 389, Boulder, CO 80309, USA

⁸Institute for Physics and Astronomy, University of Potsdam, 14476 Potsdam, Germany

⁹Astronomisches Rechen-Institut, Zentrum für Astronomie der Universität Heidelberg, Mönchhofstr. 12-14, 69120 Heidelberg, Germany

¹⁰Department of Astronomy, University of Wisconsin-Madison, 475 North Charter Street, Madison, WI 53706, USA

¹¹Institut für Astrophysik Georg-August-Universität, Friedrich-Hund-Platz 1, 37077 Göttingen, Germany

¹²Department of Physics and Astronomy, Rutgers University, 136 Frelinghuysen Road, Piscataway, NJ 08854, USA

¹³Department of Physics and Astronomy, University of North Carolina, Chapel Hill, NC 27599, USA

Accepted 2012 January 13. Received 2012 January 13; in original form 2011 December 5

ABSTRACT

We report the discovery of two new Galactic candidate luminous blue variable (LBV) stars via detection of circular shells (typical of confirmed and candidate LBVs) and follow-up spectroscopy of their central stars. The shells were detected at 22 μm in the archival data of the Mid-Infrared All Sky Survey carried out with the *Wide-field Infrared Survey Explorer* (WISE). Follow-up optical spectroscopy of the central stars of the shells conducted with the renewed Southern African Large Telescope (SALT) showed that their spectra are very similar to those of the well-known LBVs P Cygni and AG Car, and the recently discovered candidate LBV MN112, which implies the LBV classification for these stars as well. The LBV classification of both stars is supported by detection of their significant photometric variability: one of them brightened in the *R* and *I* bands by 0.68 ± 0.10 and 0.61 ± 0.04 mag, respectively, during the last 13–18 years, while the second one (known as Hen 3-1383) varies its *B*, *V*, *R*, *I* and *K_s* brightnesses by $\simeq 0.5$ – 0.9 mag on time-scales from 10 d to decades. We also found significant changes in the spectrum of Hen 3-1383 on a time-scale of $\simeq 3$ months, which provides additional support for the LBV classification of this star. Further spectrophotometric monitoring of both stars is required to firmly prove their LBV status. We discuss a connection between the location of massive stars in the field and their fast rotation, and suggest that the LBV activity of the newly discovered candidate LBVs might be directly related to their possible runaway status.

Key words: line: identification – circumstellar matter – stars: emission-line, Be – stars: evolution – stars: individual: Hen 3-1383 – stars: massive.

*Based on observations obtained with the South African Large Telescope (SALT), commissioning programmes 2010-1-RSA_OTH-001 and 2010-1-RSA_OTH-013.

†E-mail: vgvaram@mx.iki.rssi.ru

1 INTRODUCTION

Massive stars go through a sequence of transitional evolutionary stages whose duration and order are still not well established (Chiosi & Maeder 1986; Langer et al. 1994; Stothers & Chin 1996; Maeder & Meynet 2012). Of these stages, perhaps the most important in the evolutionary sense and interesting in observational manifestations is the luminous blue variable (LBV) stage (Conti 1984; Wolf 1992; Humphreys & Davidson 1994; van Genderen 2001; Vink 2009). During this stage a massive star could exhibit irregular, strong spectroscopic and photometric variability on time-scales from years to decades or longer. This variability manifests itself in changes of the stellar spectrum from that of late O/early B-type supergiants to that of A/F-type ones (e.g. Stahl & Wolf 1982; Stahl et al. 2001) and in the brightness increase by several magnitudes during the cooler (outburst) state. Major eruptions of LBV stars can masquerade as peculiar supernovae (Goodrich et al. 1989; Filippenko et al. 1995; Van Dyk, Filippenko & Li 2002; Smith et al. 2011), while some LBVs could perhaps be the direct progenitors of core-collapse supernovae (Kotak & Vink 2006; Smith et al. 2007; Gal-Yam & Leonard 2009).

The spectrophotometric variability of LBVs is often accompanied by drastic changes in the stellar mass-loss rate so that essentially all LBVs are surrounded by compact (~ 0.1 – 1 pc in diameter) shells (visible in the infrared, optical and/or radio wavebands) with a wide range of morphologies, ranging from circular to bipolar and triple-ring forms (e.g. Nota et al. 1995; Weis 2001; Smith 2007; Gvaramadze, Kniazev & Fabrika 2010c). The origin of the LBV shells can be attributed either to the interaction of stellar winds during the subsequent phases of evolution of massive stars (e.g. Robberto et al. 1993; García-Segura, Langer & Mac Low 1996) or to instantaneous ejections (e.g. Smith & Owocki 2006) caused by some catastrophic events (triggered either by internal or external factors).

The LBV phenomenon is still poorly understood, which is mostly due to the scarcity of known LBV stars (caused by the short duration, a few $\times 10^3$ – 10^4 yr, of the LBV phase). Several years ago there were only 12 confirmed Galactic members of the class and 24 candidate LBVs (cLBVs) (Clark, Larionov & Arkharov 2005; Vink 2009). The discovery of additional Galactic LBVs would, therefore, greatly advance the field and help in understanding the evolutionary status and connection of LBVs to other massive transient stars, the diversity of the environments in which they form and their distribution in the Galaxy. One can also expect that the increase of the number of known LBVs would allow us to understand the driving mechanism(s) of the LBV phenomenon and to answer the question whether a deficiency of LBVs with luminosities between $\log(L/L_\odot) \simeq 5.6$ and 5.8 is real or is a result of the small-number statistics (Smith, Vink & de Koter 2004).

A detection of LBV-like shells can be considered as an indication that their associated stars are massive and evolved (e.g. Bohannon 1997; Clark et al. 2003), and therefore could be used for selection of candidate massive stars for follow-up spectroscopy. Because of the huge interstellar extinction in the Galactic plane, the most effective channel for the detection of (circumstellar) shells is through imaging with modern infrared telescopes. The infrared imaging could also be crucial for revealing those LBV stars which are presently enshrouded in dusty envelopes created by major eruptions in the recent past and therefore are heavily obscured in the optical band. Application of this approach using the archival data of the *Spitzer Space Telescope* resulted in detection of dozens of new cLBV, blue supergiant and Wolf–Rayet (WR) stars in the Milky Way (Gvaramadze et al. 2009, 2010a,b,c; Mauerhan et al. 2010; Wachter et al.

2010, 2011; Stringfellow et al. 2012a,b). The majority of these shells are visible only in 24- μm images obtained with the Multi-band Imaging Photometer for *Spitzer* (MIPS; Rieke et al. 2004) and most of them were detected in the archival data of the 24 and 70 μm Survey of the Inner Galactic Disc with MIPS (MIPSGAL; Carey et al. 2009), which mapped 278 deg² of the inner Galactic plane ($|b| < 1^\circ$ is covered for $5^\circ < l < 63^\circ$ and $298^\circ < l < 355^\circ$, and $|b| < 3^\circ$ is covered for $|l| < 5^\circ$). The high angular resolution of the MIPS images (6 arcsec at 24 μm) even allowed us to detect a new circular shell in the Large Magellanic Cloud (LMC) and through that to discover a new WR star – the first-ever extragalactic evolved massive star detected with *Spitzer* (Gvaramadze et al. 2011a; Gvaramadze et al., in preparation).

Due to a limited sky coverage of the MIPSGAL and other *Spitzer* Legacy Programmes,¹ however, many evolved massive stars with circumstellar shells might remain undetected. The situation was somewhat improved with the recent data release of the Mid-Infrared All Sky Survey carried out with the *Wide-field Infrared Survey Explorer* (*WISE*; Wright et al. 2010).² This survey provides images at four wavelengths: 3.4, 4.6, 12 and 22 μm , with an angular resolution of 6.1, 6.4, 6.5 and 12.0 arcsec, respectively, and allows a search for infrared circumstellar shells in the regions not covered by *Spitzer*. The factor of 2 lower angular resolution of the 22- μm *WISE* data, however, makes many of the shells discovered with *Spitzer* almost indiscernible, so that we expect that only the most extended yet unknown shells would be detected with *WISE*.

In this paper, we report the discovery of two new Galactic cLBVs via detection of circular shells with *WISE* and follow-up optical spectroscopy of their central stars with the renewed Southern African Large Telescope (SALT). The new shells and their central stars are presented in Section 2. Section 3.1 describes our spectroscopic follow-up of the central stars and the data reduction. Archival and contemporary photometry of the stars is presented in Section 3.2. The obtained spectra are discussed in Section 4. The discussion is given in Section 5. We summarize and conclude in Section 6.

2 NEW CIRCULAR SHELLS AND THEIR CENTRAL STARS

Two circular shells, which are the main subject of this paper, were discovered using the *WISE* 22- μm archival data. Both shells contain central stars (see Table 4 for their coordinates), which are prominent not only in all four *WISE* wavebands but also in the optical range. We call these shells WS1 and WS2, i.e. the *WISE* shells, and, in what follows, we will use for the central stars the same names as for the associated nebulae.

Fig. 1 shows the *WISE*, Two Micron All Sky Survey (2MASS) K_s -band (Skrutskie et al. 2006) and Digitized Sky Survey II (DSS-II) red band (McLean et al. 2000) images of the field containing WS1. At 22 μm the shell is almost circular with a radius of $\simeq 35$ arcsec. One can also see an elongated (toroid-like?) region of enhanced brightness stretched within the shell in the north-west–south-east direction. The 12- μm image shows the gleam of emission probably associated with WS1 and an arc-like structure faced towards the centre of the 22- μm shell. The brightest part of this arc coincides with the region of enhanced brightness at the north-west

¹ <http://irsa.ipac.caltech.edu/Missions/spitzer.html>

² The current release of the *WISE* data covers 57 per cent of the sky.

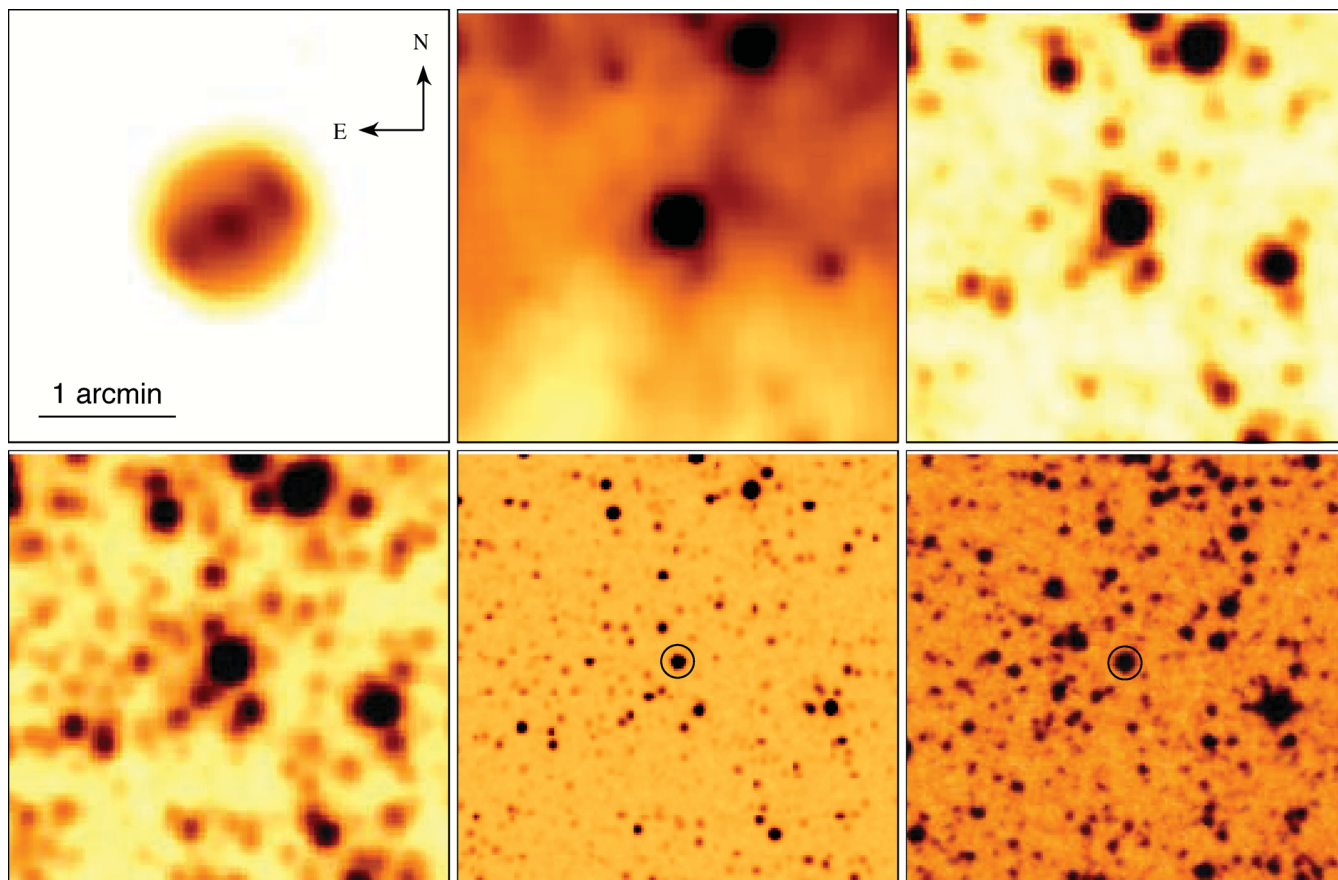


Figure 1. From left to right, and from top to bottom: *WISE* 22-, 12-, 4.6- and 3.4- μm , 2MASS K_s -band and DSS-II red band images of the circular shell WS1 and its central star (marked by a circle on the 2MASS and DSS-II images). The orientation and the scale of the images are the same.

of the shell. The central star of WS1 corresponds to the 2MASS J13362862–6345387 source (Skrutskie et al. 2006).

WS2 was discovered during our search for bow shocks generated by OB stars running away from the massive star-forming region NGC 6357 (for motivation and the results of this search, see Gvaramadze & Bomans 2008; Gvaramadze et al. 2011b, respectively). A by-product of the search, which used the archival data of the *Mid-course Space Experiment (MSX)* satellite (Price et al. 2001) and the MIPS GAL and *WISE* surveys, is the discovery of three LBV-like shells, one of which, WS2, has a central star visible in the optical region. Unfortunately, the MIPS GAL survey covers only a part of this quite extended (with a radius of ≈ 115 arcsec) shell, so that the full extent of WS2 was revealed only at 22 μm with *WISE* (see Fig. 2). The MIPS 24- μm and the *WISE* 22- μm images of WS2 have already been presented in Gvaramadze et al. (2011b).

WS2 has a clear circular limb-brightened structure with a region of reduced brightness in the south-east of the shell and a chimney-like blowup (more prominent at 24 μm due to the better angular resolution of the MIPS image) attached to a region of enhanced brightness in the north-east. The *WISE* 12- μm image shows the gleam of emission possibly related to WS2. Particularly, one can see two wings apparently extending from the central star towards the shell. One of them connects the star to the brightest part of the shell and then diverges to the ‘chimney’, while the second (less prominent) wing connects the star with the west rim of the shell. Although it is not clear whether or not these wings are related to WS2, we note that similar structures can also be seen within the

shell of the cLBV MN96 (see fig. 1(n) in Gvaramadze et al. 2010c or fig. 1 in Stringfellow et al. 2012a).

Using the SIMBAD data base³ and the VizieR catalogue access tool,⁴ we identified WS2 with the emission-line star Hen 3-1383, classified in the literature as an M3e (The 1961), an Mep? (Sanduleak & Stephenson 1973; Allen 1978) and a candidate symbiotic (Henize 1976) star. Hen 3-1383 is also known as a variable source of thermal radio emission (Seaquist & Taylor 1990; Altenhoff, Thum & Wendker 1994).

The morphology of the WS1 and WS2 shells is very similar to that of the majority of circumstellar shells associated with known (c)LBVs and related evolved massive stars (see Gvaramadze et al. 2010c), which allowed us to expect that the central stars of the shells are evolved massive stars as well. Follow-up spectroscopy of these stars confirmed our expectation and leads to the discovery of two new cLBVs.

3 OBSERVATIONS

3.1 Spectroscopic follow-up

Spectral observations of WS1 and WS2 were conducted with SALT (Buckley, Swart & Meiring 2006; O’Donoghue et al. 2006) on 11

³ <http://simbad.u-strasbg.fr/simbad/>

⁴ <http://webviz.u-strasbg.fr/viz-bin/VizieR>

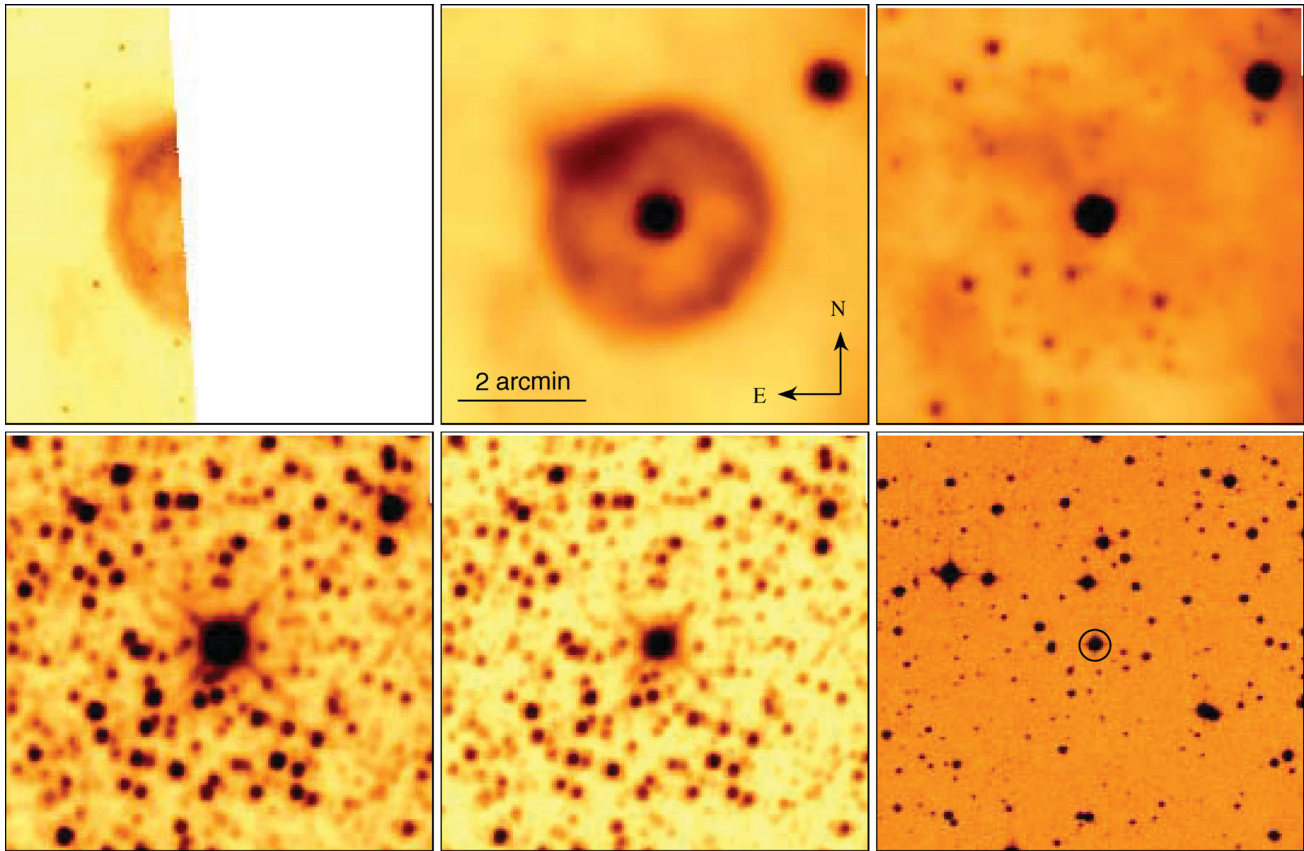


Figure 2. From left to right, and from top to bottom: *Spitzer* MIPS 24- μm , *WISE* 22-, 12-, 4.6- and 3.4- μm and DSS-II red band images of the circular shell WS2 and its central star (marked by a circle on the DSS-II image). The MIPS image is truncated because the MIPSGAL survey covers only a part of the shell. The orientation and the scale of the images are the same.

June 12 and 13 during the performance verification phase of the Robert Stobie Spectrograph (RSS; Burgh et al. 2003; Kobulnicky et al. 2003). The long-slit spectroscopy mode of the RSS was used with a 1-arcsec slit width for observations of both stars. The grating GR900 was used to cover the spectral range of 4200–7250 Å with a final reciprocal dispersion of $0.97 \text{ \AA pixel}^{-1}$ and full width at half-maximum (FWHM) spectral resolution of $4.74 \pm 0.05 \text{ \AA}$. The seeing during the observations was 2.1 arcsec for WS1 and 1.6 arcsec for WS2. Spectra of a Xe comparison arc were obtained to calibrate the wavelength scale. WS1 was observed with 3×300 s exposures, while WS2 with 2×120 and 2×600 s ones. Because of significant K_s -band photometric variability of WS2 detected in the archival data bases (see Section 3.2), we decided to re-observe this star to search for possible changes in its spectrum. A second spectrum of WS2 was taken on 2011 September 10 with 3×800 s exposures. We used the same grating to cover the spectral range of 3900–7000 Å, which allowed us to fill gaps in the wavelength coverage of the first spectrum. The seeing during this observation was variable, ≈ 3 arcsec or worse. Spectrophotometric standard stars were observed after observation of each object for relative flux calibration.

Primary reduction of the data was done with the SALT science pipeline (Crawford et al. 2010). After that, the bias- and gain-corrected and mosaicked long-slit data were reduced in the way described in Kniazev et al. (2008). The resulting rich emission-line spectra of WS1 and WS2 are presented and discussed in Section 4.

Equivalent widths (EWs), FWHMs and radial heliocentric velocities (RVs) of main emission lines in the spectra of WS1 and WS2

(measured applying the MIDAS programs; see Kniazev et al. 2004 for details) are summarized in Tables 1 and 2, respectively.

We note that SALT is a telescope with a variable pupil, so that the illuminating beam changes continuously during the observations. This makes the absolute flux/magnitude calibration impossible, even using spectrophotometric standard stars or photometric standards.

3.2 Photometry

WS2 is indicated in the International Variable Star Index (VSX) as a suspected variable with maximum visual magnitude of 12.5 (Watson 2006). Although the source of this magnitude was not indicated, we found that it comes from the paper by Sanduleak & Stephenson (1973), who estimated $V \approx 12.5$ mag as the average limiting magnitude for detection of a continuum in their low-dispersion spectra obtained with an objective prism (see also Section 5). Since Sanduleak & Stephenson (1973) did not detect the continuum in the spectrum of WS2, the actual visual brightness of this star at the moment of their observations might have been fainter than 12.5 mag. The variable status of WS2, however, can be supported by the comparison of the 2MASS and the Deep Near Infrared Survey of the Southern Sky (DENIS; The DENIS Consortium, 2005) J and K_s magnitudes (see Table 3), which shows that in 1998 the star brightened in the K_s band by $\approx 0.84 \pm 0.19$ mag during ≈ 2.5 months.

To determine the contemporary photometry of WS1 and WS2, we observed these stars with the PROMPT network, which

Table 1. EWs, FWHMs and RVs of some detected lines in the spectrum of WS1 (taken on 2011 June 12). RVs of lines noticeably affected by P Cygni absorptions are starred.

λ_0 (Å) ion	EW (λ) (Å)	FWHM (λ) (Å)	RV (km s ⁻¹)
4340 H γ	4.7 ± 0.2	4.97 ± 0.21	83 ± 6*
4471 He I	3.4 ± 0.3	8.08 ± 0.79	205 ± 22*
4554 Si III	0.5 ± 0.1	5.18 ± 0.72	198 ± 20*
4631 N II	0.2 ± 0.1	6.16 ± 0.22	102 ± 5
4658 [Fe III]	0.12 ± 0.04	6.29 ± 0.42	-103 ± 8
4686 He II	0.4 ± 0.1	10.82 ± 0.43	94 ± 8
4713 He I	1.1 ± 0.1	5.82 ± 0.19	90 ± 5
4861 H β	16.3 ± 0.3	6.53 ± 0.12	42 ± 3*
4922 He I	1.3 ± 0.2	4.52 ± 0.63	124 ± 16*
5016 He I	4.3 ± 0.2	5.98 ± 0.27	79 ± 7*
5128 Fe III	0.4 ± 0.1	4.25 ± 1.20	139 ± 30*
5156 Fe III	0.2 ± 0.1	3.33 ± 1.59	136 ± 39*
5755 [N II]	0.8 ± 0.2	8.14 ± 0.72	-41 ± 16
5834 Fe III	0.5 ± 0.2	6.65 ± 0.37	-1 ± 8
5876 He I	16.5 ± 0.5	6.29 ± 0.19	64 ± 4*
5979 Fe III	0.7 ± 0.2	6.63 ± 0.21	-16 ± 4
6000 Fe III	0.2 ± 0.1	4.06 ± 0.54	-6 ± 12
6033 Fe III	0.7 ± 0.2	6.27 ± 0.10	-14 ± 2
6347 Si II	1.3 ± 0.2	12.37 ± 0.49	-56 ± 9
6371 Si II	0.5 ± 0.1	6.84 ± 0.23	-31 ± 5
6482 N II	1.0 ± 0.1	5.98 ± 0.24	76 ± 5*
6563 H α	63.2 ± 0.9	7.86 ± 0.12	32 ± 2*
6611 N II	0.7 ± 0.1	9.13 ± 0.49	-42 ± 8
6678 He I	6.9 ± 0.3	6.27 ± 0.28	69 ± 5*
7065 He I	10.7 ± 0.3	7.20 ± 0.17	30 ± 3*

Table 2. EWs, FWHMs and RVs of some detected lines in the spectra of WS2 taken on 2011 June 13 (1) and 2011 September 10 (2). RVs of lines noticeably affected by P Cygni absorptions are starred.

λ_0 (Å) ion	EW (λ) (Å)		FWHM (λ) (Å)		RV (km s ⁻¹)	
	(1)	(2)	(1)	(2)	(1)	(2)
4340 H γ	6.92 ± 0.35	8.88 ± 0.49	6.76 ± 0.40	6.23 ± 0.40	129 ± 11*	107 ± 12*
4471 He I	3.63 ± 0.21	2.00 ± 0.07	7.01 ± 0.47	6.61 ± 0.31	134 ± 13*	76 ± 8*
4554 Si III	2.66 ± 0.10	1.52 ± 0.28	9.23 ± 0.27	8.13 ± 1.96	54 ± 8	44 ± 50
4631 N II	1.41 ± 0.05	0.66 ± 0.15	8.08 ± 0.31	7.97 ± 0.49	76 ± 7	63 ± 10
4713 He I	1.98 ± 0.05	2.20 ± 0.09	7.22 ± 0.13	7.69 ± 0.35	96 ± 3	85 ± 9
4861 H β	32.69 ± 0.56	31.61 ± 0.49	7.08 ± 0.14	7.03 ± 0.12	72 ± 4*	58 ± 3*
4922 He I	4.22 ± 0.38	-	6.21 ± 0.64	-	164 ± 17*	-
5016 He I	7.90 ± 0.45	10.71 ± 0.58	8.34 ± 0.56	8.32 ± 0.52	176 ± 14*	179 ± 13*
5128 Fe III	1.36 ± 0.10	1.45 ± 0.11	5.72 ± 0.42	6.15 ± 0.47	55 ± 11*	77 ± 12*
5156 Fe III	1.72 ± 0.07	2.12 ± 0.10	6.11 ± 0.23	6.52 ± 0.33	75 ± 6*	91 ± 8*
5171 Fe II	3.25 ± 0.09	3.55 ± 0.10	7.64 ± 0.21	8.29 ± 0.26	-36 ± 5*	-26 ± 6*
5319 Fe II	2.41 ± 0.10	2.61 ± 0.09	8.55 ± 0.20	9.82 ± 0.54	-56 ± 5	-65 ± 8
5334 [Fe II]	0.70 ± 0.11	0.65 ± 0.09	11.63 ± 0.90	9.89 ± 1.44	-24 ± 18	-40 ± 32
5376 [Fe II]	0.58 ± 0.09	0.64 ± 0.06	13.56 ± 0.32	11.25 ± 0.64	-16 ± 7	7 ± 15
5755 [N II]	2.07 ± 0.09	1.98 ± 0.08	13.11 ± 0.40	11.24 ± 0.48	-122 ± 18	-117 ± 10
5834 Fe III	0.72 ± 0.08	0.59 ± 0.19	8.72 ± 0.23	4.81 ± 1.69	21 ± 5*	-11 ± 37*
5876 He I	13.04 ± 0.26	16.42 ± 0.35	6.75 ± 0.15	7.06 ± 0.17	30 ± 3*	42 ± 4*
5979 Fe III	1.70 ± 0.09	-	10.93 ± 0.23	-	-53 ± 5	-
6000 Fe III	0.29 ± 0.06	-	7.51 ± 0.65	-	-92 ± 13	-
6033 Fe III	0.54 ± 0.05	-	6.96 ± 0.15	-	-65 ± 3	-
6347 Si II	1.43 ± 0.06	1.29 ± 0.05	9.73 ± 0.27	10.37 ± 0.30	13 ± 5*	42 ± 5*
6371 Si II	0.68 ± 0.05	0.66 ± 0.04	7.45 ± 0.12	7.49 ± 0.22	-38 ± 2	-1 ± 4
6482 N II	1.48 ± 0.20	1.50 ± 0.20	9.26 ± 1.34	9.49 ± 1.39	188 ± 26*	201 ± 27*
6563 H α	136.00 ± 2.55	108.98 ± 2.10	11.52 ± 0.25	13.73 ± 0.30	43 ± 5*	55 ± 6*
6678 He I	7.83 ± 0.45	8.37 ± 0.46	7.77 ± 0.51	7.96 ± 0.50	54 ± 10*	68 ± 10*
7065 He I	12.28 ± 0.44	-	9.17 ± 0.38	-	11 ± 7*	-
7155 [Fe II]	1.92 ± 0.16	-	16.82 ± 0.86	-	-64 ± 15	-

consists of six 0.4-m robotic telescopes operating in Chile by the University of North Carolina (Reichart et al. 2005). Observations were carried out on 2011 September 20 and 23 with the PROMPT No. 4 telescope, which is equipped with *BVRI* filters of the Johnson–Cousins photometric system. Transformations from the instrumental to the standard photometric system were obtained during several nights in 2010 using Landolt (1992) standard stars in the regions of RU 149, RU 152 and SA 98. The photometric accuracy is $\simeq 0.03$ mag in all the filters. The results are presented in Table 3, where we also give photographic magnitudes obtained from different sources and calibrated using the secondary photometric standards established from the PROMPT data, *J* and *K_s* magnitudes from 2MASS and *I*, *J* and *K_s* magnitudes from the DENIS data base.

Table 3 shows that WS1 brightened in the *I* band by 0.61 ± 0.04 mag during the last 13 years. One can also see that this brightening was accompanied by the brightness increase in the *R* band by 0.68 ± 0.10 mag. Thus, the star apparently became redder during the last 13–18 years. Similarly, Table 3 shows that WS2 became fainter in the *V* band by 0.47 ± 0.05 mag during 10 d of 2011 September, and brightened in the *I* band by 0.41 ± 0.05 mag during three months since the first spectrum was taken, i.e. the star appears to have significantly reddened on a time-scale of several months. Table 3 also shows that WS2 experienced significant (0.5–0.9 mag) variability in the *B* and *R* bands on time-scales of decades, although the poor time cadence leaves the possibility that the brightness changes in these bands occurred on much shorter time-scales.

The details of WS1 and WS2 are summarized in Table 4, where we give their 2MASS coordinates, the contemporary *B* and *V*

Table 3. Archival and contemporary photometry of WS1 and WS2.

Date	WS1					
	<i>B</i>	<i>V</i>	<i>R</i>	<i>I</i>	<i>J</i>	<i>K_s</i>
1976 March 8 ^a	17.50 ± 0.10	–	–	–	–	–
1979 June 7 ^a	–	–	–	12.60 ± 0.10	–	–
1984 February 22 ^a	–	–	14.10 ± 0.10	–	–	–
1993 June 20 ^a	–	–	14.30 ± 0.10	–	–	–
1998 July 1 ^b	–	–	–	12.79 ± 0.03	10.56 ± 0.10	8.90 ± 0.11
2000 February 22 ^c	–	–	–	–	10.33 ± 0.02	8.90 ± 0.02
2011 June 12 ^d	–	15.25 ± 0.04	–	–	–	–
2011 September 23 ^e	17.36 ± 0.03	15.31 ± 0.03	13.62 ± 0.03	12.18 ± 0.03	–	–
Date	WS2					
	<i>B</i>	<i>V</i>	<i>R</i>	<i>I</i>	<i>J</i>	<i>K_s</i>
1958 April 17 ^a	17.70 ± 0.10	–	–	–	–	–
1976 May 31 ^a	16.90 ± 0.10	–	–	–	–	–
1980 May 1 ^a	–	–	–	10.20 ± 0.10	–	–
1984 April 9 ^a	–	–	12.20 ± 0.10	–	–	–
1991 August 5 ^a	–	–	12.70 ± 0.10	–	–	–
1998 August 10 ^c	–	–	–	–	6.62 ± 0.04	4.70 ± 0.02
1998 October 29 ^b	–	–	–	9.86 ± 0.05	6.18 ± 0.12	3.86 ± 0.19
2011 June 13 ^d	–	–	–	10.13 ± 0.04	–	–
2011 September 10 ^d	–	14.10 ± 0.04	–	–	–	–
2011 September 20 ^e	17.80 ± 0.03	14.57 ± 0.03	11.89 ± 0.03	9.72 ± 0.03	–	–

^aUSNO B-1 (Monet et al. 2003); ^bDENIS; ^c2MASS; ^dSALT; ^ePROMPT.

Table 4. Details of central stars associated with two circular shells discovered with *WISE*.

	WS1	WS2 (= Hen 3-1383)
RA (J2000)	13 ^h 36 ^m 28 ^s .63	17 ^h 20 ^m 31 ^s .76
Dec. (J2000)	−63°45′38″.7	−33°09′49″.0
<i>l</i>	307.8856	353.5275
<i>b</i>	−1.3230	2.2005
<i>B</i> (mag)	17.36 ± 0.03	17.80 ± 0.03
<i>V</i> (mag)	15.31 ± 0.03	14.57 ± 0.03
[3.4] (mag)	8.03 ± 0.03	4.18 ± 0.05
[4.6] (mag)	7.59 ± 0.02	2.79 ± 0.03
[12] (mag)	6.76 ± 0.03	2.58 ± 0.02
[22] (mag)	4.62 ± 0.04	1.65 ± 0.03

magnitudes and, for the sake of completeness, the *WISE* magnitudes from the *WISE* Preliminary Release Source Catalogue.⁵

4 WS1 AND WS2 – NEW GALACTIC (CANDIDATE) LBV STARS

Figs 3–5 present the normalized spectra of WS1 and WS2 (taken on 2011 June 12 and 13, respectively) in the blue, green and red regions, where most of the identified lines are marked. For the sake of comparison, we also show in these figures the corresponding spectra of the prototype LBV P Cygni (taken from Stahl et al. 1993 and degraded to the resolution of our spectra)⁶ and the recently discovered Galactic cLBV MN112 (Gvaramadze et al. 2010b). The spectra are arranged in such a way that objects with the supposedly cooler effective temperature (see below) are placed closer to the top of the figures. One can see that all four spectra are very similar,

which suggests the LBV classification for WS1 and WS2 as well. To identify the lines indicated in the figures, we mostly used the spectral atlas of P Cygni by Stahl et al. (1993).

All four spectra are dominated by strong emission lines of H and He I; some of them show P Cygni profiles. Both H α and H β have prominent wings. Other emission lines present in all four spectra are numerous metal lines of N II, Fe III and Si II, and the carbon doublets at $\lambda\lambda$ 6578, 6583 and $\lambda\lambda$ 7231, 7236. The dichotomy of Fe III lines observed in the spectra of P Cygni (Stahl et al. 1993) and MN112 (Gvaramadze et al. 2010b) is present in the spectra of WS1 and WS2 as well: lines with low multiplet numbers (e.g. Fe III $\lambda\lambda$ 5127, 5156) have distinct P Cygni profiles, while those with higher multiplet numbers (e.g. Fe III $\lambda\lambda$ 5920–6033) are purely in emission. Some of the N II lines (e.g. $\lambda\lambda$ 6151, 6168) are also purely in emission. The only forbidden line common for all four spectra is that of [N II] λ 5755, although the presence of weak [N II] $\lambda\lambda$ 6548, 6583 lines in the H α emission wings cannot be excluded.

Numerous diffuse interstellar bands (DIBs) are present in the spectra. In the blue region they are $\lambda\lambda$ 4428, 4726 and 4762; in the green and red the strongest DIBs are at 5780, 5797, 6379 and 6613 Å. Strong absorptions visible at $\lambda > 6800$ Å are telluric. The sodium doublet in all four spectra is of interstellar origin. In addition to the interstellar lines, the spectrum of WS2 (as well as that of P Cygni; Stahl et al. 1993) shows blueshifted ($\Delta v \simeq -220$ km s^{−1}) components of circumstellar origin.

There are, however, several important distinctions in the spectra. The blue spectrum of WS1 shows the presence of a weak emission of He II λ 4686 and the high-ionization forbidden line [Fe III] λ 4658, which indicates that this star is somewhat hotter than the other three stars. The presence of these lines makes the spectrum of WS1 almost identical to that of the bona fide LBV AG Car during the epoch of a minimum in 1985–90, when it was a WN11 star (Stahl et al. 2001) with an effective temperature of $\simeq 22\,000$ – $23\,000$ K (Groh et al. 2009a). Thus, WS1 can be classified as a WN11 star. The WN11 classification of WS1 also follows from the position of this

⁵ <http://irsa.ipac.caltech.edu/cgi-bin/Gator/nph-dd>

⁶ <http://www.lsw.uni-heidelberg.de/users/ostahl/pcyg/>

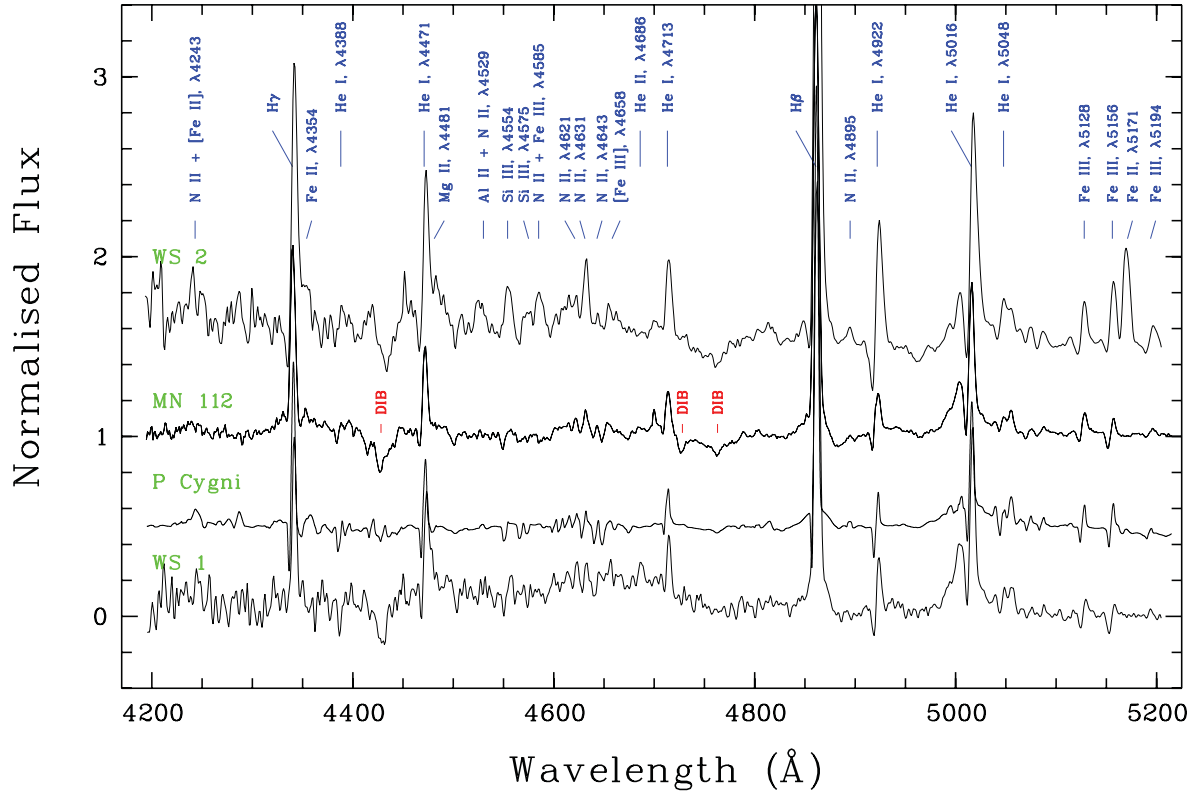


Figure 3. Comparison of normalized blue spectra of WS1 and WS2 with those of the prototype LBV P Cygni and cLBV MN112. The principal lines and most prominent DIBs are identified.

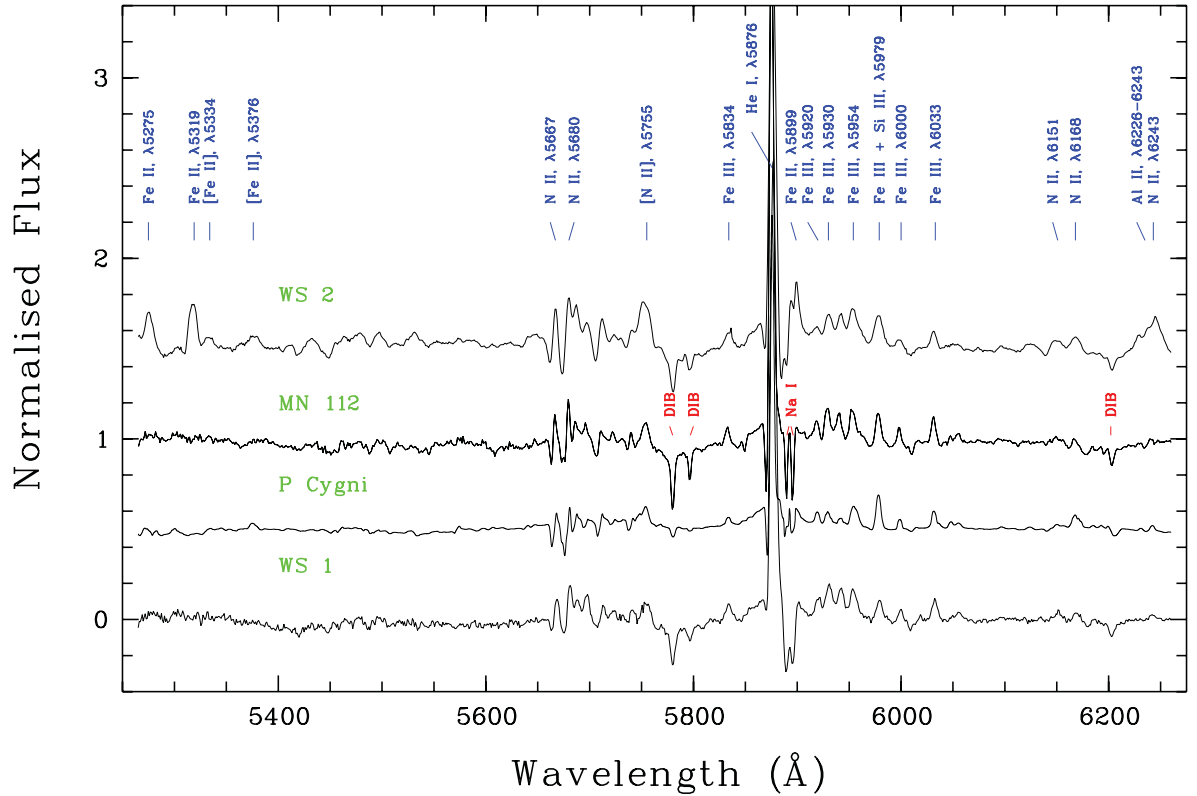


Figure 4. Comparison of normalized green spectra of WS1 and WS2 along with spectra of the prototype LBV P Cygni and cLBV MN112. The principal lines and most prominent DIBs are identified.

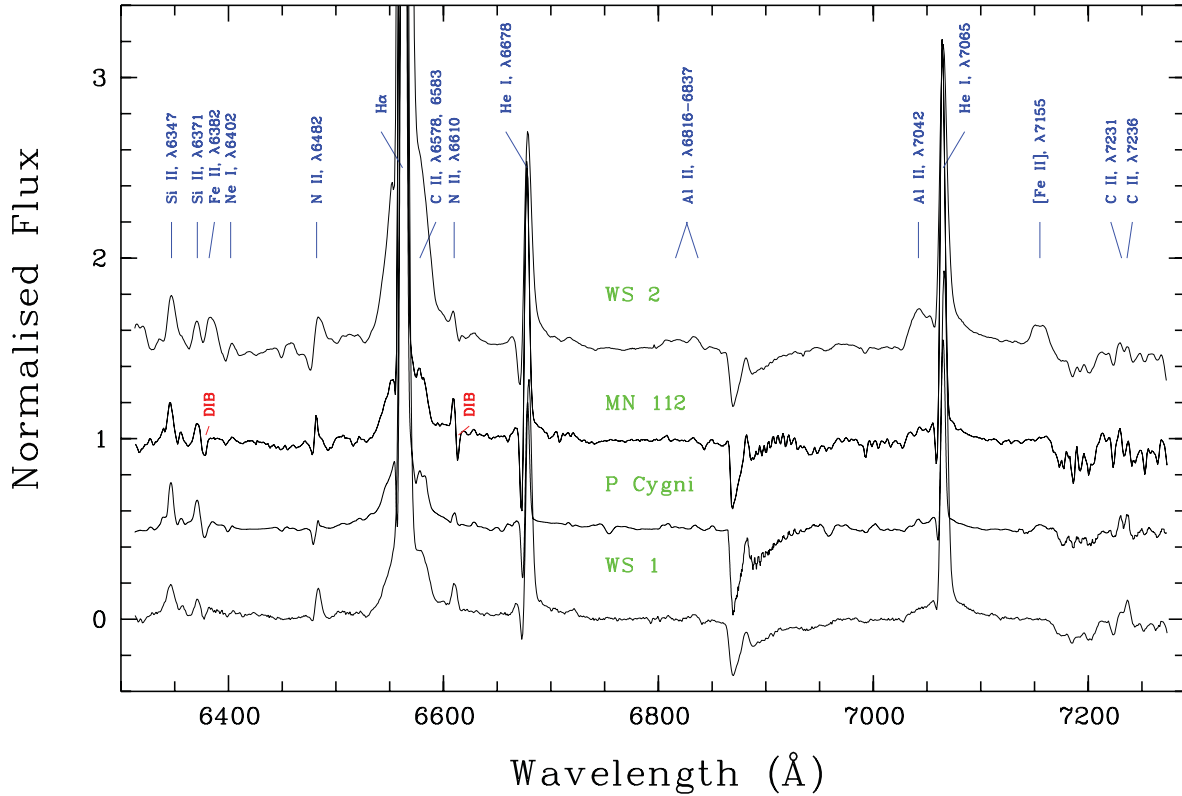


Figure 5. Comparison of normalized red spectra of WS1 and WS2 along with spectra of the prototype LBV P Cygni and cLBV MN112. The principal lines and most prominent DIBs are identified.

star on the diagrams showing a comparison of EWs of He I $\lambda 5876$ versus He II $\lambda 4686$ lines and He II $\lambda 4686$ EW versus FWHM for late WN-type (WNL) stars in the Milky Way and the LMC (see fig. 1 of Crowther & Smith 1997). With $EW(5876) = 16.5 \text{ \AA}$, $EW(4686) = 0.4 \text{ \AA}$ and $FWHM(4686) = 10.8 \text{ \AA}$ (see Table 1), WS1 lies in the region occupied by WN11 stars. We conclude, therefore, that WS1 is a cLBV near a brightness minimum.

The spectrum of WS2 shows several permitted and forbidden emission lines of singly ionized iron, which are absent or too weak to be detected in the spectra of other three stars. Of these lines the most prominent are Fe II $\lambda\lambda 5171, 5275, 5319, 5899, 6382$ and [Fe II] $\lambda\lambda 5334, 5376, 7155$. Some of the Fe II lines ($\lambda\lambda 5892\text{--}5897$) are blended with the blueshifted component of the Na I D1 line, while some others (e.g. $\lambda\lambda 4922, 5016$) are blended with the He I lines. The latter results in an anomalously high intensity ratio of He I $\lambda 4922$ to He I $\lambda 4471$ compared to the other three stars (cf. Hillier et al. 1998). Several emissions of Al II are also detected in the spectrum, of which the most prominent are at $\lambda\lambda 6226\text{--}6243$ and $\lambda 7042$. Overall, the spectrum of WS2 is very similar to those of AG Car in 2003 January (see fig. 3 in Groh et al. 2009a) and the cLBV HD 316285 (Hillier et al. 1998). Since the singly ionized iron lines appeared in the spectrum of AG Car 2 years after a visual minimum in 2001 (when the effective temperature of AG Car decreased from $\approx 17\,000$ to $14\,000 \text{ K}$; Groh et al. 2009a), one can conclude that WS2 is also near the brightness minimum and currently is either at the onset of the rise to the maximum or on the way to the minimum.

Figs 3–5 show that the emission lines of WS2 are much broader than those of WS1 (cf. also Tables 1 and 2) and the two other stars, which might be caused by a higher wind velocity, v_∞ , of WS2. Indeed, this inference is supported by measurements of the FWHM

of the [N II] $\lambda 5755$ line, which can be used as a measure of v_∞ (e.g. Crowther, Hillier & Smith 1995). After correction for instrumental width ($\approx 4.74 \pm 0.05 \text{ \AA}$), we found $v_\infty \approx 640 \pm 20 \text{ km s}^{-1}$ for WS2 and $\approx 350 \pm 40 \text{ km s}^{-1}$ for WS1. A similar value of v_∞ for WS2 also follows from the width of the flat-topped lines [Fe II] $\lambda\lambda 5334, 5376$ and 7155 : the mean value of v_∞ derived from these three lines is $\approx 690 \pm 15 \text{ km s}^{-1}$. For comparison, the wind velocities of P Cygni and MN112 are $\approx 200 \text{ km s}^{-1}$ (e.g. Barlow et al. 1994; Najarro, Hillier & Stahl 1997) and $\approx 400 \text{ km s}^{-1}$ (Gvaramadze et al. 2010b), respectively. Although the high wind velocity inferred for WS2 is more typical of WN8–9h stars (Hamann, Gräferner & Liermann 2006), we note that similar velocities were also measured for the Homunculus nebula of η Car (e.g. Allen & Hillier 1993; Meaburn, Walsh & Wolstencroft 1993) and for the LBV-like component of the WR binary HD 5980 in the Small Magellanic Cloud during its slow wind eruptive phase in 1994, when this component was transformed from a WR star in an LBV (Koenigsberger et al. 1998). This transformation was accompanied by drastic changes of the wind velocity, which reduced from ~ 3000 to 500 km s^{-1} and after the eruption increased to the initial value. Thus, it is possible that WS2 has either experienced a giant eruption in the past, so that the inferred high velocity corresponds to the polar outflow à la the Homunculus nebula, or that it is caught shortly before or soon after an LBV-like eruption, similar to what occurred in HD 5980 in 1994. In the latter case, one can expect that WS2 will show major changes in its spectrum in the near future.

To search for possible spectral variability of WS2, we obtained a second spectrum of this star ≈ 3 months after the first observation. Table 2 shows that although most lines remain invariable within their margins of error, some of them have changed their

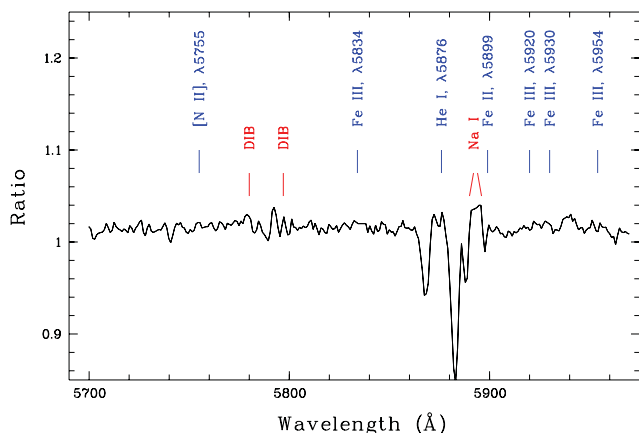


Figure 6. The ratio of the normalized (green) spectra of WS2 obtained within ≈ 3 months from each other. The positions of principal lines and most prominent DIBs are indicated.

characteristics significantly. The most noticeable changes occurred in the EWs of the He I $\lambda\lambda 5016, 5876$ lines (which became larger by ≈ 30 – 40 per cent) and in the EW and the FWHM of the H α line (which decreased and increased by ≈ 20 per cent, respectively). To illustrate these changes graphically, we divided the first normalized spectrum of WS2 by the second one. Figs 6 and 7 show the result for two spectral ranges, 5700–6000 and 6300–6750 Å, respectively. Changes in EWs, RVs and the line profiles manifest themselves in the origin of artefacts above and below continuum. Some of these artefacts show P Cygni-like profiles (e.g. at the positions of the H α and He I $\lambda 6678$ lines), while others (e.g. He I $\lambda 5876, 6678$) have an additional inverse P Cygni-like profile.

Table 2 also shows that the FWHMs of the [N II] $\lambda 5755$ and the flat-topped [Fe II] lines are systematically reduced, which indicates the reduction of the wind velocity as well. Using the FWHMs of these lines, we derived the mean wind velocity of $\approx 540 \pm 20$ km s $^{-1}$, which implies that v_{∞} decreased by $\approx 100 \pm 20$ km s $^{-1}$ during the last three months (recall that this velocity decrease is accompanied by the significant reddening of the star).

To conclude, the similarity between the spectra of WS1 and WS2 and those of the well-known LBVs P Cygni and AG Car, along with the significant short-term photometric variability, and the presence

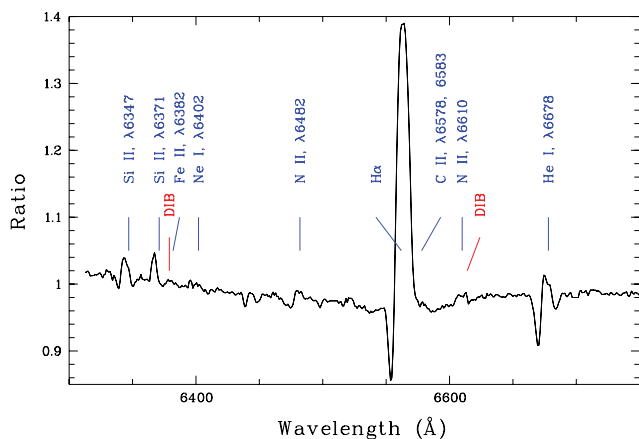


Figure 7. The ratio of the normalized (red) spectra of WS2 obtained within ≈ 3 months from each other. The positions of principal lines and most prominent DIBs are indicated.

of the circumstellar shells strongly argue for the LBV classification of both stars. For WS2, this classification is further supported by the changes in the spectrum. We hope that spectroscopic and photometric monitoring of WS1 and WS2 will allow us to confirm the LBV status of these stars in the foreseeable future.

5 DISCUSSION

5.1 Classification of WS2

We reported the detection of two circular shells with *WISE* and the results of follow-up optical spectroscopic observations of their central stars with SALT, which lead to the discovery of two new Galactic cLBVs, WS1 and WS2. WS2 was known long ago as an emission-line star Hen 3-1383 and was classified in the literature as an M-type star, which is completely discrepant with our classification of this star as a cLBV. Let us discuss the possible origin of the discrepancy.

The existing spectral classifications of WS2 were based on the observations carried out ≈ 30 – 60 yr ago, so that one can wonder whether WS2 has evolved bluewards during the last several decades. Although there are no known examples of such a radical change in the spectral type of any known star, one cannot completely exclude this possibility. For instance, in the recent past WS2 might be a yellow hypergiant star, which, like the M33's hypergiant star Var A (Humphreys, Jones & Gehrz 1987), experienced periodic changes of spectral type from pseudo-M type to G type during excursions on the cool side of the yellow void (de Jager & Nieuwenhuijzen 1997). These excursions were accompanied by episodes of enhanced mass loss due to atmospheric instability (de Jager 1998). Finally, several decades ago WS2 made a last blueward swing and after crossing the yellow void found themselves close to the S Doradus instability strip (Wolf 1989), where we currently observe it as an LBV. WS2 therefore might be a more evolved analogue of the blueward evolving yellow hypergiant IRC+10 420 (Oudmaijer 1998), which most probably will turn into an LBV in the near future (Humphreys, Davidson & Smith 2002). The characteristic time-scale of formation and dispersal of obscuring envelopes around yellow hypergiants ranges from years to decades, which is comparable to the time period elapsed between our and the previous spectroscopic observations of WS2.

The above considerations imply that WS2 has emerged as an LBV only a few decades ago. This implication, however, is inconsistent with the presence of the extended (parsec-scale; see below) circumstellar shell around this star because shells of this scale are rather typical of LBV and WNL stars, but were never observed around known yellow hypergiants (e.g. Humphreys et al. 1997; Jura & Werner 1999; Smith et al. 2001; Lagadec et al. 2011). Although one cannot exclude the possibility that WS2 became an LBV star relatively long ago and that in the recent past it experienced a giant eruption leading to the formation of an extended pseudo-photosphere, which pushed the star on the cool side of the yellow void (cf. Smith et al. 2004) and which dispersed during the last several decades, we believe that the origin of the discrepancy between the former and the present spectral classifications of WS2 is rather more prosaic. Let us discuss the sources of the previous classifications.

WS2 was identified as an emission-line star by The (1961), who found a strong H α emission in its spectrum (obtained in 1960). The (1961) classified the star as M3 and suggested that ‘it is possibly a long-period variable star’, although no information on the basis

of these findings was provided. The visual brightness of WS2 was measured to be 14 mag.

Sanduleak & Stephenson (1973) classified WS2 as a Mep? star on the basis of detection of an extremely strong H α emission (with no evidence of H β and He II λ 4686 emissions) and the suspected presence of TiO bands. WS2 does not show evidence of a continuum on the survey plates (taken in 1967–68), from which Sanduleak & Stephenson (1973) concluded that the star was fainter than 12.5 mag at that time. This magnitude is quoted in several subsequent catalogues (e.g. in Watson 2006, where the star is indicated as a possible symbiotic variable of the Z Andromedae type).

The TiO bands (and the continuum as well) were not visible in the spectrum taken in 1949–51 by Henize (1976), who interpreted the presence of the very strong H α emission as the indication that WS2 might be a symbiotic star.

The spectral classifications of WS2 given in all the three above-mentioned papers were based on objective-prism spectra. The first (low-dispersion) slit spectrum of WS2 was obtained in 1977 by Allen (1978), who suspected the presence of weak TiO absorption and tentatively classified the star as a peculiar M-type emission-line star (i.e. Mep?), because the H I and He I emissions in its spectrum ‘are very strong for an Me star’.

To summarize, the existing historical spectroscopic data show that WS2 is an emission-line star with very strong H α emission (detected in all spectra starting from 1949 till 1977) and H I emission (detected in 1977 in the first slit spectrum of the star). TiO bands were suspected in 1967–68 and 1978, and were not visible in 1949–51. Although with this information we cannot exclude the possibility that WS2 was an pseudo-M-type emission-line star \approx 30–60 yr ago, it is plausible that the previous spectral classifications are erroneous because of the low quality of the spectroscopic material, aggravated by high visual extinction ($A_V \sim 10$ mag; see below) towards the star.

5.2 Reddening towards WS1 and WS2

We now turn to estimate the reddening towards WS1 and WS2. First, we matched the dereddened spectral slopes of these stars with those of stars of similar effective temperature. Using the Stellar Spectral Flux Library by Pickles (1998) and assuming the effective temperatures of WS1 and WS2 of 22 000 and 14 000 K (see Section 4), respectively, we found the colour excess $E(B - V) = 2.40$ mag for WS1 and $E(B - V) = 3.37$ mag for WS2. These estimates only slightly depend on the assumed effective temperature. By varying the temperature in a quite wide range (\approx 12 000–260 00 K for WS1 and \approx 11 000–23 000 K for WS2), we found $E(B - V) \approx 2.37 \pm 0.10$ mag for WS1 and $E(B - V) \approx 3.36 \pm 0.10$ mag for WS2. We also compared the spectral slopes of WS1 and WS2 with that of AG Car (using the spectra of AG Car obtained by us on 2009 June 1 and 2011 May 19), and found that they nicely match each other if one dereddens the spectra of WS1 and WS2, respectively, by 1.53–1.66 and 2.61–2.73 mag in $E(B - V)$. Adopting $E(B - V) = 0.63$ mag for AG Car (Humphreys et al. 1989), we found $E(B - V) = 2.16$ –2.29 mag for WS1 and $E(B - V) = 3.24$ –3.36 mag for WS2, which agree fairly well with the above estimates.

The reddening can also be estimated by using the correlation between the intensity of the DIBs and $E(B - V)$ (see Herbig 1995, for a review). In Table 5 we provide estimates of $E(B - V)$ for both stars based on EWs of DIBs at λ 5780 and λ 5797, and the relationships given in Herbig (1993). We did not find this approach useful because of the large spread in the resulting estimates of $E(B - V)$ and their inconsistency with those derived from the spectral slopes. The

Table 5. Estimates of the colour excess, $E(B - V)$, towards WS1 and WS2 based on the EWs of DIBs at λ 5780 and λ 5797 in the spectra of these stars.

DIB (\AA)	WS1		WS2	
	EW(λ) (\AA)	$E(B - V)$ (mag)	EW(λ) (\AA)	$E(B - V)$ (mag)
5780	1.79 ± 0.22	3.38 ± 0.52	1.78 ± 0.12	3.36 ± 0.46
5797	0.83 ± 0.19	6.06 ± 0.88	0.91 ± 0.12	6.69 ± 0.85

discrepancy could be caused by foreground regions of enhanced number density of carriers of the DIBs. Another possibility is that the circumstellar material around WS1 and WS2 produces the DIB carriers and through that contributes to the strength of the DIBs⁷ (cf. Tüg & Schmidt-Kaler 1981; Heydari-Malayeri et al. 1993; Le Bertre & Lequeux 1993). In what follows we assume $E(B - V) = 2.4$ mag for WS1 and $E(B - V) = 3.4$ mag for WS2, and use these figures to constrain the distances to and the luminosities of these stars. Using the standard ratio of total to selective extinction $R_V = 3.1$, we obtained $A_V \approx 7.4$ mag for WS1 and $A_V \approx 10.5$ mag for WS2.

5.3 Location of WS1 and WS2

To estimate the distance to WS1, we use the empirical fact that LBVs in the hot state are located on the S Doradus instability strip (Wolf 1989). Assuming that the current effective temperature of WS1 is \approx 22 000–23 000 K (see Section 4), we found the minimum luminosity of this star of $\log(L/L_\odot) \approx 5.8$. Then assuming that the bolometric correction of WS1 is equal to that of AG Car during the epoch of minimum in 1985–90, -2.4 mag (Groh et al. 2009a), we found the absolute visual magnitude $M_V \approx -7.3$ mag and the distance of \approx 11 kpc (which places WS1 on the far side of the Carina–Sagittarius arm). At this distance the linear radius of the shell is \approx 1.8 pc (i.e. a figure typical of LBV shells; e.g. Weis 2001), while the distance from the Galactic plane is \approx 240 pc, which implies that WS1 is a runaway star (e.g. Blaauw 1993). The luminosity of WS1 would be higher if this star left the S Doradus instability strip and now undergoes an outburst or recovers after it. Correspondingly, the distance to the star would be larger, while its runaway status would be even more unavoidable.

In Section 2, we mentioned that WS2 was detected not far (\approx 1:4 to the north-west) from the star-forming region NGC 6357 and its associated massive star clusters Pismis 24 and AH03 J1725–34.4, which are located on the close side of the Carina–Sagittarius arm at a distance of \approx 1.7 kpc (Gvaramadze et al. 2011b). At the same time, WS2 is projected on the eastern periphery of the Sco OB4 association (see Fig. 8), which is located at a distance of \approx 1.1 kpc (Kharchenko et al. 2005). Let us discuss whether or not one of these stellar systems might be the birthplace of WS2.

The possible association of the WC7 star WR 93 with Pismis 24 (Massey, DeGioia-Eastwood & Waterhouse 2001) implies that the age of this cluster is \gtrsim 2–2.5 Myr, so that the cluster is old enough for some of its (most massive) members to enter the LBV phase. On the other hand, the \approx 40 pc separation (in projection) of WS2 from Pismis 24 would imply that WS2 is a runaway star. Assuming that WS2 was ejected from Pismis 24 and that the ejection event occurred \sim 2 Myr ago, one has the peculiar transverse velocity of

⁷ We measured the EWs of DIBs in both spectra of WS2 and found that they agree with each other within the margin of errors (see also Fig. 6).

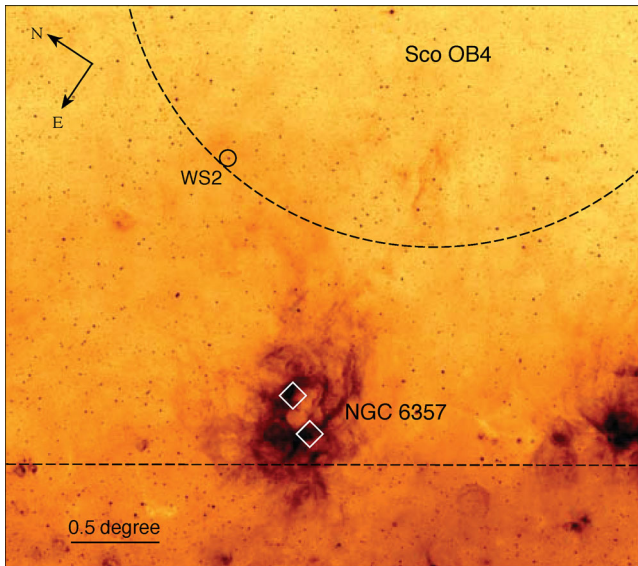


Figure 8. *MSX* 8.3- μm image of the star-forming region NGC 6357 (containing the star clusters Pismis 24 and AH03 J1725–34.4; indicated by diamonds) and its environments. The position of WS2 is marked by a small circle. The approximate boundary of the Sco OB4 association is shown by a large dashed circle. The Galactic plane is shown by a dashed line.

this star of $\simeq 20 \text{ km s}^{-1}$. The peculiar velocity of WS2, however, would be several times higher if the star was ejected less than 2 Myr ago and if its space velocity has a significant radial component. Such peculiar velocities can easily be achieved in the course of three-body dynamical encounters between very massive binary and single stars in the dense cores of young star clusters (e.g. Gvaramadze & Gualandris 2011). Detection of numerous very massive runaway stars around very young ($\sim 1\text{--}2$ Myr) massive star clusters (Evans et al. 2010; Gvaramadze, Kroupa & Pflamm-Altenburg 2010d; Bestenlehner et al. 2011; Roman-Lopes, Barba & Morrell 2011) supports the theoretical expectation that the dynamical evolution of such clusters is dominated by the most massive stars, so that the ejected stars are also preferentially the most massive ones. Unfortunately, the existing proper motion measurements for WS2 are very unreliable, so that we did not attempt to calculate its peculiar transverse velocity and thus to check its runaway status.

Assuming that the bolometric correction of WS2 is equal to that of AG Car during the epoch of minimum in 2003, -1.2 mag (Groh et al. 2009a), and adopting $V = 14.1$ mag and the distance of 1.7 kpc, we found $M_V \simeq -7.6$ mag and $\log(L/L_\odot) \simeq 5.4$.⁸ These estimates imply that WS2 might belong to a group of low-luminosity LBVs with $\log(L/L_\odot) \simeq 5.2\text{--}5.6$ (Humphreys & Davidson 1994), which in turn would imply that the progenitor of WS2 has evolved through a red supergiant stage (Humphreys & Davidson 1994; Smith et al. 2004). The latter implication, however, means that the initial mass of WS2 was $\lesssim 25\text{--}30 M_\odot$ and that its age is $\gtrsim 5$ Myr, which is inconsistent with the young age of Pismis 24, and argues against the association between these two objects.

If WS2 is a member of the Sco OB4 association ($d = 1.1$ kpc; Kharchenko et al. 2005), then $M_V \simeq -6.6$ mag and $\log(L/L_\odot) \simeq 5.1$. The resulting luminosity is therefore well below the minimum

luminosity found for any known (c)LBV and would place WS2 on the hot side of the S Doradus instability strip. Therefore, WS2 is most likely a background star projected on Sco OB4 by chance.

It is also possible that WS2 is located in one of the next two arms out, the Crux–Scutum arm or the Norma arm. In this case, the distance to WS2 is either $\simeq 3$ or 5 kpc, which corresponds to $M_V \simeq -8.8$ mag and $\log(L/L_\odot) \simeq 5.9$ or $M_V \simeq -9.9$ mag and $\log(L/L_\odot) \simeq 6.4$, respectively. Note that for P Cygni and AG Car (during the minimum phase) these parameters are equal, respectively, to -8.0 mag and 5.8 (Najarro et al. 1997) and -8.1 mag and 6.2 (Groh et al. 2009a). At the distance of 3–5 kpc, the linear radius of the shell is $\simeq 1.6\text{--}2.7$ pc, which is still within the range of radii derived for LBV shells. Placing WS2 at a larger distance, say at 8 kpc, increases its M_V and $\log(L/L_\odot)$ to $\simeq -10.9$ mag and $\simeq 6.8$, respectively. This would make WS2 the most luminous (c)LBV known to date, while its separation from the Galactic plane and the radius of the shell would be $\simeq 300$ and $\simeq 4.4$ pc, respectively. Taken together, these extreme figures make the large distances to WS2 unlikely. To conclude, we deem that the distance to WS2 is either $\simeq 3$ or 5 kpc, although we cannot exclude the possibility that WS2 was expelled from a star cluster (of appropriate age) hidden in the molecular cloud associated with the star-forming region NGC 6357 (cf. Gvaramadze et al. 2011b).

5.4 WS1 and WS2 as runaway stars

We now discuss the possibility that the LBV activity of WS1 and WS2 and their possible runaway status might be related.

The fraction of runaway O stars is found observationally to be about 10–30 per cent (Gies 1987; Stone 1991; Zinnecker & Yorke 2007). Gies (2007) summarizes the evidence for runaway O stars to often be rapid rotators. This idea is enhanced by the finding of Walborn et al. (2010, 2011) that most of the spectroscopically identified fast-rotating O stars, the On stars, are runaways or are located in the field (and therefore most probably are runaways as well; Gvaramadze et al. 2010d; Weidner et al. 2011).

Theoretically, a connection between the runaway status and fast rotation of massive stars is expected. Mass transfer in a close binary may spin up the mass receiver, which becomes a runaway star upon the supernova explosion of the mass donor (Petrovic, Langer & van der Hucht 2005; Eldridge, Langer & Tout 2011). Alternatively, rapid rotators could also be produced in the course of dynamical few-body encounters in young massive star clusters, either because of merging of two (or several) stars or due to the strong tidal interaction (Alexander & Kumar 2001). In both cases, the fast-rotating star could be ejected from the cluster (e.g. Leonard 1995; Vanbeveren et al. 2009). Moreover, dynamical encounters can also produce runaway binaries (e.g. Leonard & Duncan 1990; Kroupa 1998), which then can produce rapid rotators by mass transfer or merging.

While the physical mechanism for LBV outbursts is still unclear, there is consensus that the Eddington limit plays an important role in these events (Lamers & Fitzpatrick 1988; Smith & Conti 2008) and that the critical rotational velocity of stars near their Eddington limit becomes very small (Langer 1997, 1998). The latter fact has two important consequences. First, it implies that rotation must be important in LBV outbursts (Langer 1997; Langer, García-Segura & Mac Low 1999; Maeder & Meynet 2000), which is supported by the observation (e.g. Nota et al. 1995; Weis 2011) that the youngest LBV nebulae have a bipolar shape (note that such nebulae may become more spherical with time). Secondly, while fast rotation may not be a sufficient condition to initiate the LBV phenomenon,

⁸ Note that these estimates should be considered approximate because of the significant variability of WS2 (see Table 3).

rapid rotators are more likely to become LBVs.⁹ In stars of relatively low initial mass, fast rotation may even trigger LBV activity, i.e. such stars would not become LBVs if they were slow rotators.

In this connection, we note that tidal stripping of envelopes of evolved massive stars in close dynamical encounters might drive stars towards the Eddington limit and thereby to trigger their LBV activity. This would allow stars at the low-mass end of the range of massive stars to manifest themselves as LBVs, even if they cannot approach the Eddington limit in the course of an unperturbed evolution (cf. Smith et al. 2011). Some of these stars might also be ejected in the field.

Recently, Groh, Hillier & Damineli (2006) and Groh et al. (2009b) found that the bona fide LBVs AG Car and HR Car appear to rotate close to their break-up velocities. Groh et al. (2009b) suggested that the fast rotation is typical for all LBVs with strong variability on short (\sim decades) time-scales, while the dormant or ex-LBVs (e.g. P Cygni and HD 168625) rotate more slowly. These slowly rotating (dormant/ex-) LBVs might have been fast rotators in the past, which have lost a significant fraction of their angular momentum due to one or several episodes of violent mass ejection.

When rapid rotators are more likely to become LBVs, and rapid rotators are often runaway stars, we conclude that LBVs may often be runaway stars. This is supported by the observation that AG Car and HR Car, like many other (c)LBVs, are located in the field, i.e. far from known star clusters, and therefore are likely runaways. We thus suggest that the LBV activity of WS1 and WS2 might be directly related to their runaway status.

6 SUMMARY AND CONCLUSION

We have identified two new Galactic candidate LBVs via detection of mid-infrared circular shells with *WISE* and follow-up spectroscopy of their central stars with SALT. We have found that the spectra of both stars are very similar to those of the well-known LBVs P Cygni and AG Car (during its brightness minima in 1985–90 and 2003) and the recently discovered cLBV MN112. We have also found that both stars, which we call WS1 and WS2, show significant photometric variability. Namely, WS1 brightened in the *R* and *I* bands by 0.68 ± 0.10 and 0.61 ± 0.04 mag, respectively, during the last 13–18 years, while WS2 (known as Hen 3-1383) varies its *B*, *V*, *R*, *I* and *K_s* brightnesses by $\simeq 0.5$ – 0.9 mag on time-scales from 10 d to decades. Taken together, these findings strongly suggest that the detected objects are LBVs. The LBV classification of WS2 is also supported by the spectral variability of this star on a time-scale of $\simeq 3$ months. To corroborate that WS1 and WS2 are bona fide LBVs, it is necessary to detect the major changes in their brightness ($\gtrsim 1$ – 2 mag) and spectra. Further spectroscopic and photometric monitoring of these stars is therefore warranted. We have discussed a connection between the location of massive stars in the field and their fast rotation, and suggested that the LBV activity of WS1 and WS2 might be directly related to their possible runaway status.

To conclude, careful examination of the archival data of the *WISE* survey and the *Spitzer* Legacy programmes will undoubtedly lead to new interesting discoveries, which hopefully will advance our understanding of the LBV phenomenon.

⁹ Note that the fast-rotating runaway stars might also be the progenitors of long gamma-ray bursts (Hammer et al. 2006; Cantiello et al. 2007; Eldridge et al. 2011; Le Floch et al. 2011).

ACKNOWLEDGMENTS

We are grateful to P. Morris (the referee) for his comments on the manuscript. All SAAO and SALT co-authors acknowledge the support from the National Research Foundation (NRF) of South Africa. This work has made use of the NASA/IPAC Infrared Science Archive, which is operated by the Jet Propulsion Laboratory, California Institute of Technology, under contract with the National Aeronautics and Space Administration, the SIMBAD data base and the VizieR catalogue access tool, both operated at CDS, Strasbourg, France.

REFERENCES

- Alexander T., Kumar P., 2001, *ApJ*, 549, 948
 Allen D. A., 1978, *MNRAS*, 184, 601
 Allen D. A., Hillier D. J., 1993, *Proc. Astron. Soc. Australia*, 10, 338
 Altenhoff W. J., Thum C., Wendker H. J., 1994, *A&A*, 281, 161
 Barlow M. J., Drew J. E., Meaburn J., Massey R. M., 1994, *MNRAS*, 268, L29
 Bestenlehner J. M. et al., 2011, *A&A*, 530, 14
 Blaauw A., 1993, in Cassinelli J. P., Churchwell E. B., eds, *ASP Conf. Ser. Vol. 35, Massive Stars: Their Lives in the Interstellar Medium*. Astron. Soc. Pac., San Francisco, p. 207
 Bohannan B., 1997, in Nota A., Lamers H. J. G. L. M., eds, *ASP Conf. Ser. Vol. 120, Luminous Blue Variables: Massive Stars in Transition*. Astron. Soc. Pac., San Francisco, p. 120
 Buckley D. A. H., Swart G. P., Meiring J. G., 2006, *Proc. SPIE*, 6267, 32
 Burgh E. B., Nordsieck K. H., Kobulnicky H. A., Williams T. B., O'Donoghue D., Smith M. P., Percival J. W., 2003, *Proc. SPIE*, 4841, 1463
 Cantiello M., Yoon S.-C., Langer N., Livio M., 2007, *A&A*, 465, L29
 Carey S. J. et al., 2009, *PASP*, 121, 76
 Chiosi C., Maeder A., 1986, *ARA&A*, 24, 329
 Clark J. S., Egan M. P., Crowther P. A., Mizuno D. R., Larionov V. M., Arkharov A., 2003, *A&A*, 412, 185
 Clark J. S., Larionov V. M., Arkharov A., 2005, *A&A*, 435, 239
 Conti P. S., 1984, in Maeder A., Renzini A., eds, *Observational Tests of the Stellar Evolution Theory*. Reidel, Dordrecht, p. 233
 Crawford S. M. et al., 2010, *Proc. SPIE*, 7737
 Crowther P. A., Smith L. J., 1997, *A&A*, 320, 500
 Crowther P. A., Hillier D. J., Smith L. J., 1995, *A&A*, 293, 172
 de Jager C., 1998, *A&AR*, 8, 145
 de Jager C., Nieuwenhuijzen H., 1997, *MNRAS*, 290, 50
 Eldridge J. J., Langer N., Tout C. A., 2011, *MNRAS*, 414, 3501
 Evans C. J. et al., 2010, *ApJ*, 715, L74
 Filippenko A. V., Barth A. J., Bower G. C., Ho L. C., Stringfellow G. S., Goodrich R. W., Porter A. C., 1995, *AJ*, 110, 2261
 Gal-Yam A., Leonard D. C., 2009, *Nat*, 458, 865
 García-Segura G., Langer N., Mac Low M.-M., 1996, *A&A*, 305, 229
 Gies D. R., 1987, *ApJS*, 64, 545
 Gies D. R., 2007, in St-Louis N., Moffat A. F. J., eds, *ASP Conf. Ser. Vol. 367, Massive Stars in Interacting Binaries*. Astron. Soc. Pac., San Francisco, p. 325
 Goodrich R. W., Stringfellow G. S., Penrod D. G., Filippenko A. V., 1989, *ApJ*, 342, 908
 Groh J. H., Hillier D. J., Damineli A., 2006, *ApJ*, 638, L33
 Groh J. H., Hillier D. J., Damineli A., Whitelock P. A., Marang F., Rossi C., 2009a, *ApJ*, 698, 1698
 Groh J. H. et al., 2009b, *ApJ*, 705, L25
 Gvaramadze V. V., Bomans D. J., 2008, *A&A*, 490, 1071
 Gvaramadze V. V., Gualandris A., 2011, *MNRAS*, 410, 304
 Gvaramadze V. V. et al., 2009, *MNRAS*, 400, 524
 Gvaramadze V. V., Kniazev A. Y., Hamann W.-R., Berdnikov L. N., Fabrika S., Valeev A. F., 2010a, *MNRAS*, 403, 760
 Gvaramadze V. V., Kniazev A. Y., Fabrika S., Sholukhova O., Berdnikov L. N., Cherepashchuk A. M., Zharova A. V., 2010b, *MNRAS*, 405, 520

- Gvaramadze V. V., Kniazev A. Y., Fabrika S., 2010c, MNRAS, 405, 1047
- Gvaramadze V. V., Kroupa P., Pflamm-Altenburg J., 2010d, A&A, 519, A33
- Gvaramadze V. V., Chené A.-N., Kniazev A. Y., Schnurr O., 2011a, in Robert C., St-Louis N., Drissen L., eds, Four Decades of Research on Massive Stars, A Scientific Meeting in the Honour of Anthony Moffat (San Francisco: ASP), preprint (arXiv:1110.0126)
- Gvaramadze V. V., Kniazev A. Y., Kroupa P., Oh S., 2011b, A&A, 535, A29
- Hamann W.-R., Gräfener G., Liermann A., 2006, A&A, 457, 1015
- Hammer F., Flores H., Schaerer D., Dessauges-Zavadsky M., Le Floc'h E., Puech M., 2006, A&A, 454, 103
- Henize K. G., 1976, ApJS, 30, 491
- Herbig G. H., 1993, ApJ, 407, 142
- Herbig G. H., 1995, ARA&A, 33, 19
- Heydari-Malayeri M., Grebel E. K., Melnick J., Jorda L., 1993, A&A, 278, 11
- Hillier D. J., Crowther P. A., Najarro F., Fullerton A. W., 1998, A&A, 340, 483
- Humphreys R. M., Davidson K., 1994, PASP, 106, 1025
- Humphreys R. M., Jones T. J., Gehrz R. D., 1987, AJ, 94, 315
- Humphreys R. M., Lamers H. J. G. L. M., Hoekzema N., Cassatella A., 1989, A&A, 218, L17
- Humphreys R. M. et al., 1997, AJ, 114, 2778
- Humphreys R. M., Davidson K., Smith N., 2002, AJ, 124, 1026
- Jura M., Werner M. W., 1999, ApJ, 525, L113
- Kharchenko N. V., Piskunov A. E., Röser S., Schilbach E., Scholz R.-D., 2005, A&A, 438, 1163
- Kniazev A. Y., Pustilnik S. A., Grebel E. K., Lee H., Pramskij A. G., 2004, ApJS, 153, 429
- Kniazev A. Y. et al., 2008, MNRAS, 388, 1667
- Kobulnicky H. A., Nordsieck K. H., Burgh E. B., Smith M. P., Percival J. W., Williams T. B., O'Donoghue D., 2003, Proc. SPIE, 4841, 1634
- Koenigsberger G., Auer L. H., Georgiev L., Guinan E., 1998, ApJ, 496, 934
- Kotak R., Vink J. S., 2006, A&A, 460, L5
- Kroupa P., 1998, MNRAS, 298, 231
- Lagadec E., Zijlstra A. A., Oudmaijer R. D., Verhoelst T., Cox N. L. J., Szczerba R., Mékarnia D., van Winckel H., 2011, A&A, 534, L10
- Lamers H. J. G. L. M., Fitzpatrick E. L., 1988, ApJ, 324, 279
- Landolt A. U., 1992, AJ, 104, 340
- Langer N., 1997, in Nota A., Lamers H., eds, ASP Conf. Ser. Vol. 120, Luminous Blue Variables: Massive Stars in Transition. Astron. Soc. Pac., San Francisco, p. 83
- Langer N., 1998, A&A, 329, 551
- Langer N., Hamann W.-R., Lennon M., Najarro F., Pauldrach A. W. A., Puls J., 1994, A&A, 290, 819
- Langer N., García-Segura G., Mac Low M.-M., 1999, ApJ, 520, L49
- Le Bertre T., Lequeux J., 1993, A&A, 274, 909
- Le Floc'h E., Charmandaris V., Gordon K., Forrest W. J., Brandl B., Schaerer D., Dessauges-Zavadsky M., Armus L., 2011, ApJ, preprint (arXiv:1111.1234)
- Leonard P. J. T., 1995, MNRAS, 277, 1080
- Leonard P. J. T., Duncan M. J., 1990, AJ, 99, 608
- McLean B. J., Greene G. R., Lattanzi M. G., Pirene B., 2000, in Manset N., Veillet C., Crabtree D., eds, ASP Conf. Ser. Vol. 216, Astronomical Data Analysis Software and Systems IX. Astron. Soc. Pac., San Francisco, p. 145
- Maeder A., Meynet G., 2000, A&A, 361, 159
- Maeder A., Meynet G., 2012, Rev. Mod. Phys., 84, 25
- Massey P., DeGioia-Eastwood K., Waterhouse E., 2001, AJ, 121, 1050
- Mauerhan J. C., Wachter S., Morris P. W., Van Dyk S. D., Hoard D. W., 2010, ApJ, 724, L78
- Meaburn J., Walsh J. R., Wolstencroft R. D., 1993, A&A, 268, 283
- Monet D. G. et al., 2003, AJ, 125, 984
- Najarro F., Hillier D. J., Stahl O., 1997, A&A, 326, 1117
- Nota A., Livio M., Clampin M., Schulte-Ladbeck R., 1995, ApJ, 448, 788
- O'Donoghue D. et al., 2006, MNRAS, 372, 151
- Oudmaijer R. D., 1998, A&AS, 129, 541
- Petrovic J., Langer N., van der Hucht K. A., 2005, A&A, 435, 1013
- Pickles A. J., 1998, PASP, 110, 863
- Price S. D., Egan M. P., Carey S. J., Mizuno D. R., Kuchar T. A., 2001, AJ, 121, 2819
- Reichart D. E. et al., 2005, Nuovo Cimento C, 28, 767
- Rieke G. H. et al., 2004, ApJS, 154, 25
- Robberto M., Ferrari A., Nota A., Paresce F., 1993, A&A, 269, 330
- Roman-Lopes A., Barba R. H., Morrell N. I., 2011, MNRAS, 416, 501
- Sanduleak N., Stephenson C. B., 1973, ApJ, 185, 899
- Seaquist E. R., Taylor A. R., 1990, ApJ, 349, 313
- Skrutskie M. F. et al., 2006, AJ, 131, 1163
- Smith N., 2007, AJ, 133, 1034
- Smith N., Conti P. S., 2008, ApJ, 679, 1467
- Smith N., Owocki S. P., 2006, ApJ, 645, L45
- Smith N., Humphreys R. M., Davidson K., Gehrz R. D., Schuster M. T., Krautter J., 2001, AJ, 121, 1111
- Smith N., Vink J. S., de Koter A., 2004, ApJ, 615, 475
- Smith N. et al., 2007, ApJ, 666, 1116
- Smith N., Li W., Silverman J. M., Ganeshalingam M., Filippenko A. V., 2011, MNRAS, 415, 773
- Stahl O., Wolf B., 1982, A&A, 110, 27
- Stahl O., Mandel H., Wolf B., Gaeng Th., Kaufer A., Kneer R., Szeifert Th., Zhao F., 1993, A&AS, 99, 167
- Stahl O., Jankovics I., Kovacs J., Wolf B., Schmitz W., Kaufer A., Rivinius T., Szeifert T., 2001, A&A, 375, 54
- Stone R. C., 1991, AJ, 102, 333
- Stothers R. B., Chin C.-W., 1996, ApJ, 468, 842
- Stringfellow G. S., Gvaramadze V. V., Beletsky Y., Kniazev A. Y., 2012a, in Drissen L., St-Louis N., Robert C., Moffat A. F. J., eds, Four Decades of Research on Massive Stars: A Scientific Meeting in Honour of Anthony Moffat (San Francisco: ASP), preprint (arXiv:1112.2686)
- Stringfellow G. S., Gvaramadze V. V., Beletsky Y., Kniazev A. Y., 2012b, in Richards M., Hubený I., eds, Proc. IAU Symp. 282, From Interacting Binaries to Exoplanets: Essential Modeling Tools, preprint (arXiv:1112.2685)
- The DENIS Consortium, 2005, VizieR Online Data Catalog, 2263, 0
- The P.-S., 1961, Contr. Bosscha Observ. Lembang., 10, 1
- Tüg H., Schmidt-Kaler T., 1981, A&A, 94, 16
- Van Dyk S. D., Filippenko A. V., Li W., 2002, PASP, 114, 700
- Van Genderen A. M., 2001, A&A, 366, 508
- Vanbeveren D., Belkus H., van Bever J., Mennekens N., 2009, Ap&SS, 324, 271
- Vink J. S., 2009, preprint (arXiv:0905.3338)
- Wachter S., Mauerhan J. C., van Dyk S. D., Hoard D. W., Kafka S., Morris P. W., 2010, AJ, 139, 2330
- Wachter S., Mauerhan J., van Dyk S., Hoard D. W., Morris P., 2011, Bull. Soc. R. Sci. Liège, 80, 322
- Walborn N. R. et al., 2010, AJ, 139, 1283
- Walborn N. R., Maíz Apellániz J., Sota A., Alfaro E.J., Morrell N. I., Barbá R. H., Arias J. I., Gamen R. C., 2011, AJ, 142, 150
- Watson C. L., Henden A. A., Price A., 2006, in Warner B. D. et al., eds, Society for Astronomical Sciences Annual Symposium Vol. 25, The International Variable Star Index (VSX). SAS, Rancho Cucamongo, CA, p. 47
- Weidner C., Gvaramadze V. V., Kroupa P., Pflamm-Altenburg J., 2011, in Stellar Clusters and Associations (A RIA workshop on GAIA, 23-27 May 2011, Granada, Spain), preprint (arXiv:1111.0294)
- Weis K., 2001, Rev. Modern Astron., 14, 261
- Weis K., 2011, Bull. Soc. R. Sci. Liège, 80, 322
- Wolf B., 1989, A&A, 217, 87
- Wolf B., 1992, Rev. Modern Astron., 5, 1
- Wright E. L. et al., 2010, AJ, 140, 1868
- Zinnecker H., Yorke H. W., 2007, ARA&A, 45, 481

This paper has been typeset from a $\text{\TeX}/\text{\LaTeX}$ file prepared by the author.